Monthly Notices
of the
ROYAL ASTRONOMICAL SOCIETY

Mon. Not. R. Astron. Soc. **402,** 2666–2670 (2010) doi:10.1111/j.1365-2966.2009.16083.x

The comoving infrared luminosity density: domination of cold galaxies across $0 < z < 1$

N. Seymour,[1⋆] M. Symeonidis,[1] M. J. Page,[1] M. Huynh,[2] T. Dwelly,[3] I. M. M^{c}Hardy[3] and G. Rieke[4]

[1]*Mullard Space Science Laboratory, UCL, Holmbury St Mary, Dorking, Surrey, RH5 6NT*
[2]*Infrared Processing and Analysis Center, MS220-6, California Institute of Technology, Pasadena, CA 91125, USA*
[3]*School of Physics & Astronomy, University of Southampton, Highfield, Southampton SO17 1BJ*
[4]*Steward Observatory, Tucson, 85721, USA*

Accepted 2009 November 20. Received 2009 November 13; in original form 2009 August 7

ABSTRACT

In this paper, we examine the contribution of galaxies with different infrared (IR) spectral energy distributions (SEDs) to the comoving IR luminosity density (IRLD), a proxy for the comoving star formation rate (SFR) density. We characterize galaxies as having either a *cold* or *hot* IR SED depending on whether the rest-frame wavelength of their peak IR energy output is above or below 90 μm. Our work is based on a far-IR selected sample both in the local Universe and at high redshift, the former consisting of *IRAS* 60 μm-selected galaxies at $z < 0.07$ and the latter of *Spitzer* 70 μm selected galaxies across $0.1 < z \leq 1$. We find that the total IR luminosity densities for each redshift/luminosity bin agree well with results derived from other deep mid-/far-IR surveys. At $z < 0.07$, we observe the previously known results that moderate luminosity galaxies ($L_{IR} < 10^{11}\,\mathrm{L}_{\odot}$) dominate the total luminosity density and that the fraction of cold galaxies decreases with increasing luminosity, becoming negligible at the highest luminosities. Conversely, above $z = 0.1$, we find that luminous IR galaxies ($L_{IR} > 10^{11}\,\mathrm{L}_{\odot}$), the majority of which are cold, dominate the IRLD. We therefore infer that cold galaxies dominate the IRLD across the whole $0 < z < 1$ range, hence appear to be the main driver behind the increase in SFR density up to $z \sim 1$ whereas local luminous galaxies are not, on the whole, representative of the high-redshift population.

Key words: galaxies: evolution – galaxies: starburst – infrared: galaxies.

1 INTRODUCTION

The rise in the comoving star formation rate (SFR) density up to $z \sim 1$ and its subsequent flattening (Lilly et al. 1996; Madau et al. 1996) has now been well studied at several wavelengths (e.g. Bunker et al. 2004; Hopkins & Beacom 2006, and references therein). While the global picture to $z = 1$ has been well constrained by the observation, the details of how or why this change occurs remain largely unknown. There now is evidence that star formation depends on both galaxy mass (Feulner et al. 2005; Juneau et al. 2005) and environment (Lewis et al. 2002; Elbaz et al. 2007) presenting a more complicated picture of galaxy evolution than simple evolution of the luminosity function.

The infrared (IR), and particularly the far-IR, is one of the most powerful tracers of star formation as IR luminosity directly scales with SFR (Kennicutt 1998, and references therein) and far-IR emission originates from the regions of cold dust and gas that constitute the fuel for an on-going burst of star formation. Another advantage of selecting sources at long wavelengths is the low contribution by active galactic nuclei (AGN), if present, to the total IR luminosity (Alexander et al. 2003; Clements et al. 2008). Studies of the distant Universe at IR wavelengths remain limited and the most sensitive probe has been surveys with the *Spitzer* 24 μm band. However, this wavelength is relatively far from the peak of all but the hottest IR galaxies and progressively shifts to shorter wavelengths at higher redshifts where strong spectral features in the observed frame can also complicate matters. The few studies done with deep *Spitzer* 70 μm imaging have found rapid evolution in the total IR luminosity function (Huynh et al. 2007; Magnelli et al. 2009). When the IR luminosity function is integrated at different redshifts it is found that the IR luminosity density (IRLD) increases rapidly up to $z = 1$ in a similar fashion to the SFR density. Nevertheless, the relative contribution by luminosity to the IRLD changes with redshift with starbursts [$10 \leq \log(L_{IR}/\mathrm{L}_{\odot}) < 11$] dominating locally, but with luminous IR galaxies [LIRGs: $11 \leq \log(L_{IR}/\mathrm{L}_{\odot}) < 12$] and

⋆E-mail: nseymouruk@gmail.com

ultraluminous IR galaxies [ULIRGs: $12 \leq \log(L_{IR}/L_{\odot}) < 13$] becoming increasing contributors at higher redshifts (Le Floc'h et al. 2005; Magnelli et al. 2009).

In Symeonidis et al. (2009, hereafter S09) we studied the IR spectral energy distributions (SEDs) of a sample of 70 μm selected galaxies at $z \geq 0.1$, using a sample of local, $z < 0.1$, *IRAS* 60 μm selected galaxies for comparison. We fitted the mid- to far-IR photometry of both samples with models from Siebenmorgen & Krügel (2007). We found that the majority of the 70 μm sources had IR SEDs which peaked, in $\nu \times F_{\nu}$, at longer wavelengths than galaxies from the local sample with similar luminosities. In the local sample, we observed a shift of the IR SED peak to shorter wavelengths with increasing luminosity (as has previously been noted, Sanders & Mirabel 1996; Chapman et al. 2003; Rieke et al. 2009), whereas the 70 μm sample had a wide range of peak wavelengths the distribution of which varied little with luminosity. The observation that the IR SEDs of luminous, distant galaxies were on average different to their local analogues was in contrast to other recent results, Magnelli et al. (e.g. 2009) who concluded that there was no significant change in IR SED of luminous galaxies with redshift. Models of galaxy evolution in the IR have tended to assume that the SEDs of high-redshift luminous sources follow the luminosity trend seen in local sources (Lagache, Puget & Dole 2005; Pearson 2005; Le Borgne et al. 2009; Rowan-Robinson 2009). However, as shown in S09, the range of IR SEDs for luminous galaxies is much wider at high redshifts than seen locally.

In this paper, we examine the contribution of galaxies with different IR SEDs to the comoving IRLD. We will compare our results to earlier work (Le Floc'h et al. 2005) by examining the contribution to the IRLD by luminosity, but this time with a sample selected at 70 μm rather than 24 μm. This selection enables us to use a more robust selection of IR luminous galaxies as 70 μm lies closer to the peak of typical IR SEDs. Hence, the total IR luminosity can also be estimated more accurately, especially with constraints (mainly detections) from 160 μm data. We examine the IRLD in more detail by focusing on the contribution by IR SED type within each bin. By obtaining an estimate of the peak of the IR SED in rest-frame $\nu \times F_{\nu}$, we can characterize these IR bright sources as being either *cold* or *hot* depending on whether the SED peaks above or below 90 μm (32.2 K for a blackbody). We choose this wavelength for two reasons. First, local IR galaxies appear to have a warm IR component ($\bar{\lambda} \sim 60$ μm) associated with dust around young star-forming regions and a cooler 'cirrus' component ($\lambda \geq 100$ μm) associated with more extended dust heated by the interstellar radiation field (Lonsdale & Helou 1987). Secondly, this 90 μm cut also marks a divide between the SEDs of most local ULIRGs and those of cold sub-millimeter galaxies (SMGs) seen at high redshift, most of which would be classified as cold by our definition (Chapman et al. 2005). We note that there is a linear relationship between the *IRAS* colours often used to define the IR galaxies as 'cold' or 'hot' (e.g. Chapman et al. 2003) and the peak wavelength used in this work.

We present our far-IR galaxy sample in Section 2, describe our determination of the comoving IRLD in Section 3. We present our results in Section 4 and discuss them in Section 5. Throughout this paper, we use the current 'concordance' cosmology: $\Omega_{\rm M} = 1 - \Omega_{\Lambda} = 0.3, \Omega_0 = 1$ and $H_0 = 70\,{\rm km\,s^{-1}\,Mpc^{-1}}$ (Spergel et al. 2003).

2 THE FAR-IR GALAXY SAMPLE

The IR luminous galaxies we use here are taken from the study of S09 who used a local and distant far-IR selected sample. The local sample is the *IRAS* Bright Galaxy Sample (BGS) from Sanders et al. (2003), which is selected to have 60 μm flux densities above 5.24 Jy covering the entire sky surveyed by *IRAS* at Galactic latitudes $|b| > 5^{\circ}$. The higher redshift sample we use consists of *Spitzer* 70 μm galaxies from two well-studied extragalactic fields: the Extended Groth Strip (EGS covering ∼0.°3; Davis et al. 2007) and the $13^{\rm H}$ *XMM–Newton/Chandra Deep Field* ($13^{\rm H}$ covering ∼0.°3; Seymour et al. 2008).

We restrict our 70 μm sample to sources with $0.1 \leq z \leq 1.0$ ruling out local resolved sources at $z < 0.1$ and very high redshift sources where there may not be complete redshift information. Although the $13^{\rm H}$ field 70 μm sample has complete redshift information (40 spectroscopic and 40 photometric) the original EGS spectroscopic survey only targeted ∼2/3 of candidate sources (Davis et al. 2007). By examining the original EGS 70 μm sample (Symeonidis et al. 2007), we estimate from broad-band colours that 101 sources lie within $0.1 \leq z \leq 1.0$, 66 of which have spectra. Hence, in the next section, we multiply the area of the EGS by a factor of 66/101 to correct for those sources not included on the assumption these 66 are representative of the parent population. We impose a further cut of $S_{70\mu{\rm m}} > 10$ mJy, to remove lower signal-to-noise sources where we are not complete, leaving us with 123 sources in our 70 μm sample from both fields.

We use the total IR luminosities and peak wavelengths determined in S09 which were derived from fits to models from Siebenmorgen & Krügel (2007). These models were fit to photometry at 12, 25, 60 and 100 μm for the local sample and at 8, 24, 70 and 160 μm for the *Spitzer* 70 μm sample. The IR luminosity–redshift distribution for both samples is plotted in Fig. 1, where we have characterized each source as having a cold or hot IR SED depending whether it peaks above or below our fiducial wavelength of 90 μm.

3 METHOD

We determine the IRLD using a version of the classic $1/V_{\rm max}$ method (Schmidt 1968; Felten 1976). We use the following formula to determine the luminosity density in each redshift/luminosity bin

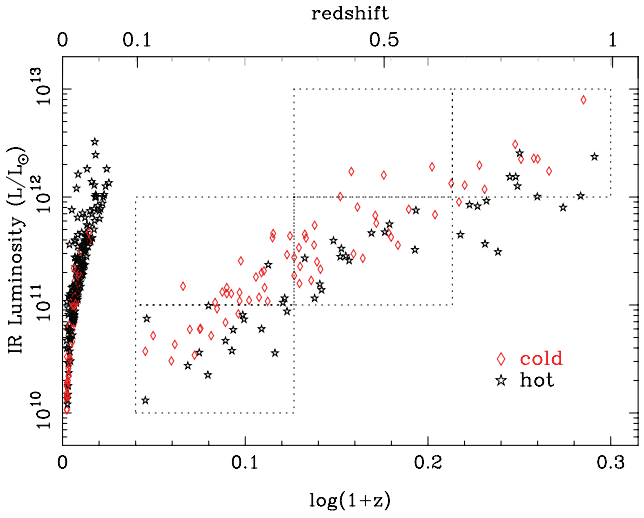

Figure 1. The redshift/total (8–1000 μm) IR luminosity distribution of the local ($z < 0.07$) BGS sample and our *Spitzer* 70 μm sample ($z > 0.1$) with sources characterized as cold or hot depending on whether their IR SED peaks above or below 90 μm (rest-frame in $\nu \times F_{\nu}$). The dotted lines indicate the binning chosen to investigate the comoving IRLD by IR luminosity and SED.

for the 70 μm sample

$$\Phi_{\rm IR}(L, z) = \Sigma_i(L_i/V_i), \quad (1)$$

where L_i is the total 8–1000 μm IR luminosity (in solar units) of a source and V_i is the maximum volume (in Mpc^3) a source could occupy given the size of the redshift bins, the area of the survey, our 10 mJy completeness limit and the best-fitting SED as determined in S09. The same method was used for the local BGS sample, also using the best-fitting SED found in S09, but the V_i was limited by the 5.24 Jy detection limit at 60 μm and a redshift range of $0.005 \leq z \leq 0.07$. Uncertainties are determined using the expression:

$$\delta\Phi_{\rm IR}(L, z) = \sqrt{\Sigma_i(L_i/V_i)^2 + \delta\Phi(\delta L_i)^2}, \quad (2)$$

where V_i and L_i are defined as before and the $\delta\Phi(\delta L_i)$ term represents the contribution of the uncertainty in the luminosity of individual sources within that bin (due to photometric redshifts and the modelling in S09). The binning (see Fig. 1) was defined by the definitions of the luminosity class (ULIRG etc.) and the desire to have bins of equal size in $\log(1+z)$ space, i.e. approximately equal epochs in cosmic time. We do not include a bin to cover the highest redshift LIRGs as our survey is much less sensitive to cold galaxies in this region of parameter space and hence we are unable to derive a representative ratio of hot and cold galaxies. For each luminosity–redshift bin, we calculated the total comoving IRLD as well as that for the cold and hot galaxies separately. The redshift used when plotting each bin is the mean redshift of all the sources contributing to that bin in $\log(1+z)$ space. Upper limits for a bin with no cold or hot sources were determined from the 97.72 per cent confidence limit (equivalent to 2σ) for a null detection (Gehrels 1986) using the volume of the whole bin and the mean luminosity of all the galaxies in the bin.

In S09, we discussed how the construction of our sample might affect the results. The selection of the 70 μm sample at rest-frame 35–60 μm means our selection could potentially favour galaxies that peak around those wavelengths, i.e. hot galaxies by our definition, contrary to the increasing fraction of cold galaxies. We also established that the uncertainty in the long-wavelength *Spitzer*/160 μm photometry did not have a significant effect on the peak wavelength determined from the SED fitting. The uncertainties on IR luminosity from the SED fitting, when carried over to this work, contribute little to the total uncertainties on individual data points in Fig. 2, i.e. small number statistics dominate.

4 RESULTS

We present the observed comoving IRLD of our sample in Fig. 2 as a function of luminosity and redshift. The total IR luminosity densities at each luminosity–redshift bin are in good agreement with those from Le Le Floc'h et al. (2005) notwithstanding the potential sample variance between small volumes and the different IR SED models used. The results presented here also broadly agree with those of Magnelli et al. (2009) who base their work on stacking 24 μm selected sources at longer wavelengths. The largest disagreement with previous work is at $z \sim 0.2$ where the total IRLD of the starbursts presented here is about 0.4 dex below the value of Le Floc'h et al. (2005).

Examining the contribution by IR SED to each luminosity–redshift bin, we find that there is significant variation in the relative contribution of cold and hot galaxies with luminosity and redshift. Locally, we see cold sources dominating the starburst bin, but at higher luminosities they contribute less; cold galaxies comprise only one-third of the LIRG bin and they contribute nothing to the ULIRG bin. The contribution of cold galaxies to the IRLD from starbursts remains fairly constant at 60–70 per cent over the redshift range we can detect them, $0 \leq z \leq 0.2$. However, for both LIRG and ULIRG bins, the contribution from cold galaxies increases considerably at higher redshifts. Cold galaxies become the dominant contributor to the IRLD in these bins above $z = 0.1$, in contrast to the situation seen in the local Universe. In fact, cold galaxies are responsible for most of the rise with redshift of the IRLD in both the LIRG and ULIRG bins.

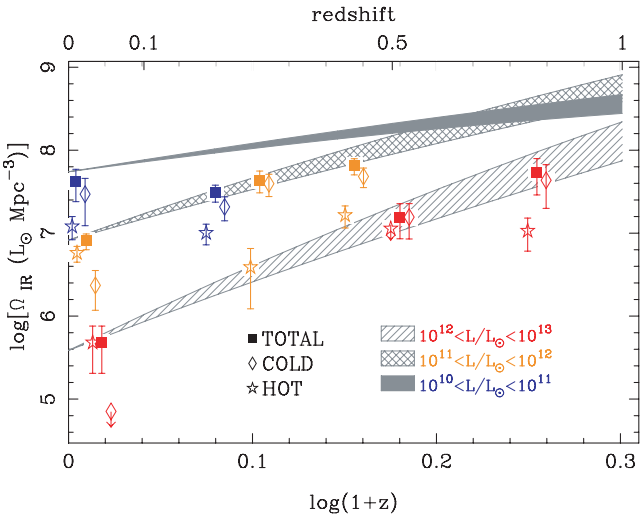

Figure 2. The comoving IRLD plotted as a function of redshift in different luminosity bins: starbursts (blue), LIRGs (yellow) and ULIRGs (red). For each bin, we plot the total IRLD and the separate contribution from the cold and hot galaxies. The hot and cold points are marginally offset in redshift from the total IRLD for clarity. Derivation of the uncertainties and upper limits (representing null detections) is explained in the text. Locally ($z < 0.1$) we use the *IRAS* BGS and at other redshifts we use the *Spitzer* 70 μm selected sample from S09. We overlay, for comparison, the IRLD derived from deep 24 μm observations by Le Floc'h et al. (2005, shaded regions). We observe a general trend of hot galaxies dominating the local LIRG and ULIRG bins, but the increase in IRLD at higher redshifts is mainly due to an increase in the contribution from cold galaxies rather than hot galaxies.

In Fig. 3, we plot the fraction of the total IRLD in each redshift/luminosity bin due to cold galaxies. We can see how the contribution of cold galaxies to the starburst luminosity density remains constant up to $z \sim 0.2$, although our data here cannot constrain that fraction at higher redshifts. The contribution of cold galaxies to the LIRG and ULIRG luminosity density increases dramatically with redshift; locally the contribution is very low or negligible, but at higher redshift cold galaxies dominate. We find that our results do not change qualitatively if we change our choice of fiducial wavelength (that divides between hot or cold galaxies) by ±10 μm.

5 DISCUSSION

In S09, we demonstrated that the IR SEDs of individual LIRGs and ULIRGs at $0.1 \leq z \leq 1.0$ peak at longer wavelengths, and span a wider range, than local galaxies at similar luminosities. Other changes in the properties of star-forming galaxies have occurred since $z \sim 1$. Star formation shifts from massive galaxies at high redshifts to progressively less massive galaxies at lower redshifts (e.g. Cowie et al. 1996; Juneau et al. 2005). A shift is also seen in environment of the most strongly star-forming galaxies with

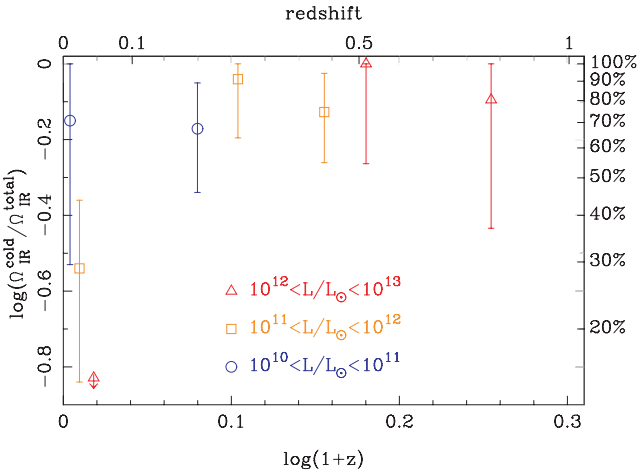

Figure 3. The fraction of the comoving IRLD for different redshift/luminosity bins due to cold galaxies ($\lambda_{peak} > 90$ μm) also given as a percentage on the right axis. Note by this definition we have no cold galaxies in our local ULIRG sample.

star formation tending to occur in overdense environments at $z \sim 1$ (Elbaz et al. 2007), a reverse of the trend seen locally. While the dependence of star formation on stellar mass and environment inform us about the star formation history and potential or current galaxy mergers, information about the IR SED is a direct measure of the physical conditions in galaxies underlying major episodes of star formation.

In this paper, we have expanded the results of S09 by deriving IR luminosity densities at different luminosities and epochs. We observe that the total IR luminosity densities derived from a 70 μm sample are broadly consistent with results derived from shorter wavelengths (Fig. 2). The low IRLD of the $z \sim 0.2$ starburst bin compared to other results is likely due to the effect of sample variance over the small cosmic volume probed. We also separate our sample into galaxies that can be characterized as having cold or hot SEDs and study their contribution to each redshift/luminosity bin. We find two striking new results. First, we observed a rapid change in the make up of LIRG and ULIRG bins: locally they are dominated by hot galaxies, but at $z > 0.2$ they are dominated by cold galaxies. Secondly, cold galaxies appear to be the dominant contributor to the total IRLD over $0 \leq z \leq 1.0$; when starburst galaxies dominate at $z < 0.2$ we find that they are mainly cold and by the time LIRGs and ULIRGs begin to dominate at higher redshifts they are also mainly cold. Hence, a cold mode of star formation has dominated galaxy evolution since $z \sim 1$ and is likely responsible for the increase in the SFR density up to $z = 1$.

While Fig. 2 does dramatically show the rise of cold galaxies in the LIRG and ULIRG bins at higher redshifts, we note that hot galaxies are still found at those redshifts. In fact the results presented here do not rule out a rise with redshift in the number (and luminosity density) of hot galaxies. Therefore, the distribution of types of SEDs remains quite wide at high redshift. Fig. 3 most strikingly demonstrates the evolution of the relative contribution of cold galaxies to each redshift/luminosity bin. The rise in the contribution of cold galaxies to the LIRG and ULIRG bins is most rapid between $z \sim 0$ and 0.3. We now consider if AGN could be responsible for the change in the fraction of cold galaxies. As a powerful AGN would make the IR SED hotter, the presence of an AGN cannot explain the prevalence of cold galaxies at high redshift. AGN could, however, be the cause of the high fraction of hot galaxies locally. Studies have shown that the incidence of AGN is low in local LIRGs, 10–20 per cent, (Petric et al., in preparation), but while it is higher in ULRIGs, ∼40 per cent (Farrah et al. 2007) the 8–1000 μm IR luminosity remains dominated by star formation. We note that at higher redshift the incidence of AGN, and their contribution to total IR luminosity, also remains low (Alexander et al. 2003; Clements et al. 2008). Hence, AGN are not a significant contributor to the IR luminosity of the sources studied here and therefore are not responsible for any of the trends with redshift.

The prominence of cold galaxies discovered here might suggest that there could be a substantial contribution to the IR emission of luminous galaxies at high redshift from a cold cirrus component akin to that observed in local IR galaxies. Such an interpretation is in agreement with the observation that many of the distant, cold, SMGs are extended on scales of ∼10 kpc (Chapman et al. 2004) in contrast with the compact ULIRGs seen locally, and is also consistent with the change in the mean IR SED of luminous galaxies as inferred from the observed 70 μm to radio flux density ratio of high redshift star-forming galaxies (Seymour et al. 2009). In addition, changes in dust properties (such as opacity, grain distribution etc.) with redshift are also a possible cause of the larger spread in SED types at high redshift.

Most galaxy evolution models (e.g. Lagache et al. 2005; Pearson 2005; Le Borgne et al. 2009; Rowan-Robinson 2009) assume that the IR SED is only dependent on IR luminosity, i.e. they typically use certain templates for star-forming galaxies of a given luminosity, often using local galaxies like Arp 220 (which can be characterized as having a hot IR SED by our definition) for the most luminous population. This choice was often necessary as there were few constraints on any change with redshift until now. Models based on cooler SEDs could , for example, reconcile the flat or decreasing SFR density above $z = 1$ and the far-IR and sub-millimetre source counts.

In conclusion, we have found that the star formation history of the Universe is dominated by cold galaxies across $0 < z < 1$ and that the hot luminous IR galaxies we see locally are not representative of the luminous galaxies that make up the bulk of the star formation at $0.1 < z < 1$.

ACKNOWLEDGMENTS

We thank Andrew Hopkins for useful discussions. This work is based in part on observations made with the *Spitzer Space Telescope*, which is operated by the Jet Propulsion Laboratory, California Institute of Technology under a contract with NASA. Support for this work was provided by NASA through an award issued by JPL/Caltech. The National Radio Astronomy Observatory is a facility of the National Science Foundation operated under cooperative agreement by Associated Universities, Inc. This work was partially supported by JPL/Caltech contract 1255094 to the University of Arizona.

REFERENCES

Alexander D. M. et al., 2003, AJ, 126, 539
Bunker A. J., Stanway E. R., Ellis R. S., McMahon R. G., 2004, MNRAS, 355, 374
Chapman S. C., Helou G., Lewis G. F., Dale D. A., 2003, ApJ, 588, 186
Chapman S. C., Smail I., Windhorst R., Muxlow T., Ivison R. J., 2004, ApJ, 611, 732
Chapman S. C., Blain A. W., Smail I., Ivison R. J., 2005, ApJ, 622, 772
Clements D. L. et al., 2008, MNRAS, 387, 247

Cowie L. L., Songaila A., Hu E. M., Cohen J. G., 1996, AJ, 112, 839
Davis M. et al., 2007, ApJ, 660, L1
Elbaz D. et al., 2007, A&A, 468, 33
Farrah D. et al., 2007, ApJ, 667, 149
Felten J. E., 1976, ApJ, 207, 700
Feulner G., Gabasch A., Salvato M., Drory N., Hopp U., Bender R., 2005, ApJ, 633, L9
Gehrels N., 1986, ApJ, 303, 336
Hopkins A. M., Beacom J. F., 2006, ApJ, 651, 142
Huynh M. T., Frayer D. T., Mobasher B., Dickinson M., Chary R.-R., Morrison G., 2007, ApJ, 667, L9
Juneau S. et al., 2005, ApJ, 619, L135
Kennicutt R. C. Jr, 1998, ApJ, 498, 541
Lagache G., Puget J.-L., Dole H., 2005, ARA&A, 43, 727
Le Borgne D., Elbaz D., Ocvirk P., Pichon C., 2009, A&A, 504, 727
Le Floc'h E. et al., 2005, ApJ, 632, 169
Lewis I. et al., 2002, MNRAS, 334, 673
Lilly S. J., Fevre O. L., Hammer F., Crampton D., 1996, ApJ, 460, L1
Lonsdale C. J., Helou G., 1987, ApJ, 314, 513
Madau P., Ferguson H. C., Dickinson M. E., Giavalisco M., Steidel C. C., Fruchter A., 1996, MNRAS, 283, 1388
Magnelli B., Elbaz D., Chary R. R., Dickinson M., Le Borgne D., Frayer D. T., Willmer C. N. A., 2009, A&A, 496, 57
Pearson C., 2005, MNRAS, 358, 1417
Rieke G. H., Alonso-Herrero A., Weiner B. J., Pérez-González P. G., Blaylock M., Donley J. L., Marcillac D., 2009, ApJ, 692, 556
Rowan-Robinson M., 2009, MNRAS, 394, 117
Sanders D. B., Mazzarella J. M., Kim D.-C., Surace J. A., Soifer B. T., 2003, AJ, 126, 1607
Sanders D. B., Mirabel I. F., 1996, ARA&A, 34, 749
Schmidt M., 1968, ApJ, 151, 393
Seymour N. et al., 2008, MNRAS, 386, 1695
Seymour N., Huynh M., Dwelly T., Symeonidis M., Hopkins A., McHardy I. M., Page M., Rieke G., 2009, MNRAS, 397, 1728
Siebenmorgen R., Krügel E., 2007, A&A, 461, 445
Spergel D. et al., 2003, ApJS, 148, 175
Symeonidis M. et al., 2007, ApJ, 660, L73
Symeonidis M., Page M. J., Seymour N., Dwelly T., Coppin K., McHardy I., Rieke G. H., Huynh M., 2009, MNRAS, 397, 1728 (S09)

This paper has been typeset from a TEX/LATEX file prepared by the author.